Novel blade-free turbomachine concept for microgasturbine engine applications

(Part 1. Design. Design characteristics. Metal model realization)

A.Soudarev[1], A.Souryaninov[1], V.Tikhoplav[1], A.Molchanov[1], P.Avran[2], L.Lelait[3]

[1] Boyko Research-Engineering "Ceramic Heat Engine" Center, Polustrovsky av., 15, block 2, St.Petersburg, RUSSIA,
Phone: +7 812 225 34 53, FAX: +7 812 225 34 53, E-mail:soudarev@boykocenter.spb.ru
[2] Engineer Consultant,Expert for l'Ecole Normale Supérieure de Paris,15 rue du Fort,91120,Palaiseau, France
Phone: +33683677596, FAX: +33160142830, E-mail:patrick.avran@minitel.net
[3] European Institute For Energy Research,Technologiepark,Emmy Noether Strasse,11,Karlsruhe,Germany
Phone: 4972161051315, E-mail:laurent.lelait@edf.fr

ABSTRACT

The recent cut-clear trend **to decentralize** the power and heat power supply to the industrial and agricultural sites, utilities, health care buildings, hotels, etc has widened the microgasturbine engine (**microGTE**) market dramatically with demand increasing tens times . This is due, primarily, to **very low emissions** of toxic substances from the microGTE exhausts, low **maintenance expenses, high startup characteristics** within a wide range of the ambient temperatures, etc. At the same time, **the microGTE efficiencies are lower** those of the **piston engines** which makes increasing the efficiency an especially burning task, particularly, as applied to the microGTEs of the 5 to 100KW power range. A way to solve the task could be the blade-free turbomachine concept, e.g. tunnel turbines which description is below (Patent of France,2002). The like design must provide increase in the efficiency of the turbine or compressor stage both through increasing its internal efficiency and a reasonable use of the structural ceramic materials to manufacture the uncooled flow passage of the turbine. The numerical gas-dynamic studies performed demonstrated that the efficiency of the tunnel channels is 0.75-0.80. By now, a test rig was designed and manufactured to study the gas-dynamic characteristics of the tunnel turbomachines. Experiments will be carried out soon with their results presented at this congress.

INTRODUCTION

A reason which prompts decreasing the efficiency of the gasturbine engines with their downscaling is a dramatic increasing in their complexity (with very small sizes) and **impracticability of cooling** for parts and components of the high-temperature path of the microGTE, especially of the **rotor blades and guide vanes of turbine** which is the most loaded and essential element of an engine as it determines its efficiency and operation reliability. Therefore, it is necessary **either** to limit the initial temperature value at the turbine inlet up to (**TIT< 850-900ºC**) which allows the uncooled metal turbine stages to operate reliably **or** switch over to application of **structural and composite materials** to manufacture high-temperature elements. Use of ceramic structural materials (SCMs) in the flow passages of the engines allows a substantial increasing the initial gas temperature at the turbine inlet. Due to this, the efficiency of a plant increases notably higher a similar metal structure since parts and components of SCMs do not require cooling (Gabrielsson,1998, Price,1999, Tatsumi,1999). The latter approach is generally embodied in the form similar to the metal microGTEs, where the most loaded elements (primarily, rotor blades) are exposed to the effects of the **tensile and bending loads.** This, in turn, allows to increase TIT up to 1300 – 1500 ^{0}C with the adequate increasing the microGTE efficiency, the latter achieved by having no cooling power losses, on the one hand, and a notable **operation reliability** of ceramic parts and components of microGTE, on the other hand, with, therefore, making their destruction less plausible.

Another reason to decrease the internal efficiency of the turbine and compressor stages for microGTE is a **greater leak and overleak percentage** of the working media in turbomachines (turbine, compressor) between the rotor and stator through gaps which relative height increases with decreasing the representative sizes of the rotor blades and guide vanes of the turbomachines.

1.Objective of developments

The objective of the present study is the research-engineering substantiation and practical embodiment of the like design of stages for turbomachine of microGTE that ensures:

-feasibility of a reliable operation of stator and rotor elements under high temperature conditions without cooling application;

-reducing inner losses in the stage imposed by leaks and overleaks of the working media along the gaps between the stator and rotor elements;

-increasing the adaptability to manufacture and decreasing the manufacture cost for stages compared with the conventional designs of axial and radial turbomachines.

2.Tunnel turbomachine concept and its advantageous specific features

A burning challenge of the current gasturbomachinery industry is to produce reliable high-temperature elements of the gasturbine engine (GTE), first and foremost, the nozzle vanes and rotor blades of high-temperature gas turbines, using structural ceramics. The compression strength of the structural ceramics (SCMs) is essentially higher the tensile one. This prompted designers to look for gas turbine rotor designs where the rotor blades exposed to the centrifugal forces effects would rather compress than stretch.

A variety of concrete design approaches allowing theoretically to put the like concept into effect are available in literature. These approaches could be subdivided as follows:

-bell-shaped rotor with blades on their internal surface (Elkins,1999), they are ordinary "drum" type rotors having the lowest admissible peripheral velocity and, therefore, the lowest mass and overall sizes;

-disc-type turbine wheels with stressed shroud that encircles the rotor blades over the periphery and absorbs the centrifugal loads to which it is exposed;

-rotor including the support metal elements and compressing the ceramic elements at operation and, also, the axial turbine rotor blades for ceramic gasturbine engines based on this operating principle (Soudarev,2002);

-the sectional turbine wheels of the radial turbines (Dietz, 1989) where segments of the ceramic rotor blades made integral with the tails are abutting against the cooled edge along the disc periphery that absorbs effects imposed by the centrifugal forces, furthermore, the centrifugal forces of the mass proper of the tail and blade are absorbed partially by the lateral conic surface of the inclined platform of the turbine wheel disc. The latter design has proved itself the most successful for the microGTE and nanomachines application. Though it has some faults, namely, first, limitation of the peripheral velocity due to an insufficient strength of thin rotor blades and wheel due to the inclination of its disc platform towards the rotor blade segments and, secondly, as a consequence, limitation of the expansion operation in the turbine.

Use of the radial gas turbine in the small power plants is preferable compared with the axial design both from the point of view of simplicity and, in some cases, the arrangement streamlining, and due to better adaptability to control, lesser aerodynamic losses at low working media flows. At the same time, given the peripheral supply of hot combustion products over the turbine disc circumference, and in the plane normal to the longitudinal axis of the engine, it seems impracticable to place the ceramic elements in the turbine disc to create predominantly the compression loads at rotation, eliminating thereat a decrease in the reliability at high values of the peripheral velocity. Though, the repeated analysis of the structures above mentioned revealed that the like approach on the basis of turbomachine tunnel structures is feasible.

The tunnel turbine (Fig.1) stage is the annular guide vanes and turbine wheel disc inside which **3-D channels** (tunnels) are envisaged, they replace the interblade channels of the turbine stages having axial or radial blades .

The total number of the tunnel channels in the turbomachine stage disc is split to some **alternating sets of different geometry** which allows to attain the optimum stressed state exposed to the thermal and mechanical loads through providing the thickness of baffles between tunnels that would correspond to the strength values required over their entire length.

For high-temperature microGTE, when application of the metal materials becomes inadequate due to high cooling losses, the tunnel designs with internal **ceramic lining** operating under complex stressed state at rotation, though with the **prevailing effect of the compressive loads,** become **the most appropriate.** Thus, you can increase its efficiency not decreasing at the same time its operation reliability.

Another benefit of the tunnel design of turbomachines is their **high adaptability to manufacture** and, therefore, **low manufacture cost.** Actually, the tunnel turbomachine stage includes, besides fastening parts, three elements, namely one stator (turbine nozzle vanes or compressor diffuser) and two rotor elements (turbine or compressor composed disc)

machined using 5-coordinate N/C machine. It allows not only to **speed up** the process of manufacture of the tunnel turbomachines and **to make it cheaper** but, also, to provide its **high precision**, so much required to ensure a reliable operation of microGTE.
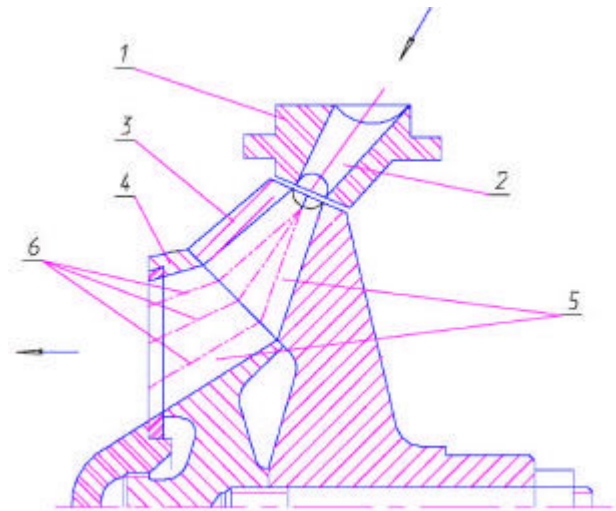

Fig.1 Tunnel turbine stage
1 – annular nozzle vanes, 2 – nozzle tunnel,
3 – peripheral disc for turbine wheel, 4 – preaxial disc for turbine wheel, 5 – rotor tunnels, 6 – axial lines projections of various groups with alternating geometry for rotor tunnels.

3.Tunnel turbine design

The high-temperature gas stream supplies from the GTE combustor into the system of fixed asymmetrical conic channels-tunnels made in the ceramic ring (Fig.2).

They constitute a spatial annular system of the nozzle vanes where expansion and pressure and temperature decreasing occurs.

Through the nozzle vanes , gas flows to the flow passage of the turbine wheel which is a circular rotating system of the operating tunnels having as well the configuration of cone with rectilinear axis (Fig.3).

The turbine wheel consists of two discs that are connected over the conic surface. When the tunnel axis crosses this conic surface it suffers a discontinuity and the gas stream changes its direction. Thus, as the working media flows, the rotating tunnel in the given concrete case is formed by two successive conic channels placed at an angle to one another.

In general, the turbine wheel is a hybrid metal-ceramic structure where discs made of metal and walls of the conic channels made inside are protected against a direct contact with hot gas by the ceramic sleeves. The nozzle vanes and conic sleeves are made of the heat resistant structural ceramic material that ensures a reliable operation of the tunnel turbine at a high gas temperature without high power losses induced by the turbine metal parts cooling.

The ceramic sleeves having the reverse cone configuration are pressed to the conic surface by the centrifugal forces imposed by their own mass at rotation of the turbine wheel, this conic surface being a limitation for the rotating operating tunnel. As a result, the predominantly compression stresses are generated in the sleeves favorable for the structural ceramics. According to this, a high reliability of the tunnel centripetal turbine and its high efficiency are ensured.

In the annular gap between the sleeve and channel surfaces, deflectors with the distancing semi-spherical bulges

are located, this, if required, allows build-up of an additional internal cooling of the discs.
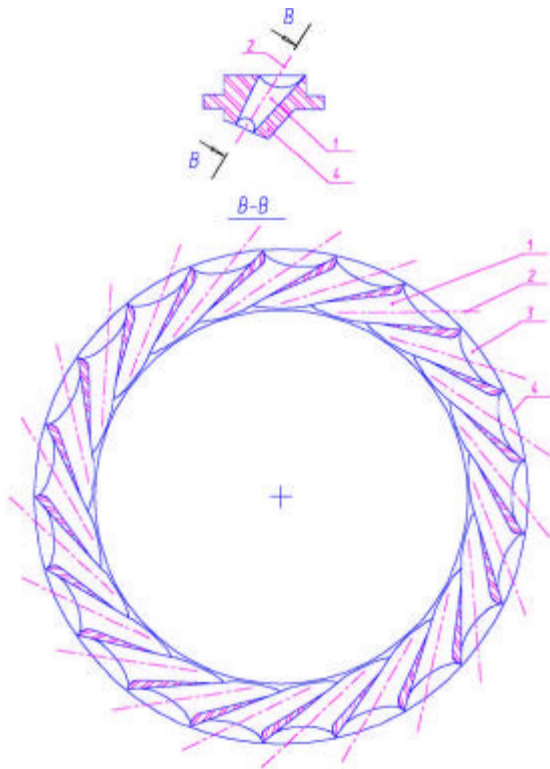

a)

b)

Fig. 2 Tunnel turbine nozzle vanes

a) meridian section of nozzle vanes and circular system for tunnels; b) aluminum model of nozzle vanes for 60 KW tunnel turbine.

1 - tunnel channel; 2 – direct axis of nozzle vanes; 3 – space formed by opening facet at nozzle tunnel inlet; 4 – ceramic ring.
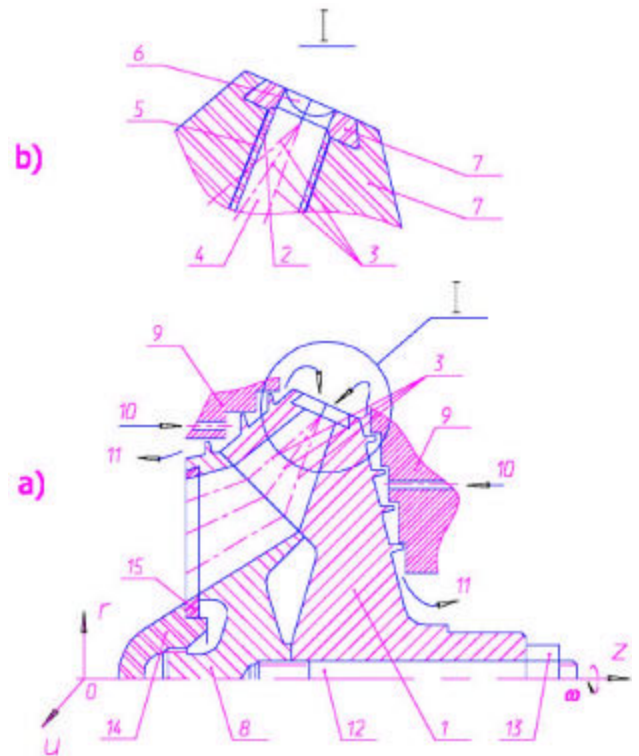

Fig. 3 Tunnel turbine wheel

a) meridian section of turbine wheel; b) inlet at peripheral disc rotor tunnel (component I)

ORUZ – coordinate system, W – speed of turbine rotor; 1 – peripheral disc of turbine wheel; 2 – ceramic conic sleeve; 3 – straight lines from groups of rotor tunnels; 4 – rotating tunnel; 5 – deflector; 6 – space formed by inlet opening face; 7 – ceramic overstructure; 8 – preaxial disc for turbine wheel; 9 – stator elements; 10 – cooling air input; 11 – cooling air output; 12, 13 – stud and nut connecting turbine wheel discs; 14 – ceramic shell; 15 - ceramic overstructure.

4.Experimental ring. Test program. Thermo-dynamical calculations.

The final goal of the operation performed is to study microGTE in complex with the tunnel ceramic turbine stage including the thermal-technical tests at rating, maximum, partial, transit, startup and shutdown duties; thermo-cyclic, life and other kinds of tests. EDF has a test rig that allows to carry out testing of microGTE of effective power up to 60KW.

The test program envisages, first, performing "cold" tests aiming to verify the gas-dynamic calculation results for the tunnel turbine stage (Fig.4.) and to estimate the polytropic efficiency of its flow passage. To develop the turbine wheel for the plant with N=60KW at the rated gas temperature at the turbine inlet T_0^*=1623K, the cycle calculation with heat regeneration was carried out aiming to opt for a pressure ratio in the cycle. Given the available heat drop in the turbine is rather high for the single-stage centripetal turbine $H_{t\ ad}^* = 518 \cdot 10^3$ J and needs in the high peripheral velocities U_1>600 m/s on the disc periphery, the pressure ratio in the cycle is selected to be π_c^*=4. The cycle scheme is in Fig.5 with parameters by nodal points, the base-line data and calculation results are in Table 1.

It should be noted that the turbine in the given calculations is conditionally subdivided into two turbines: one has power equal to the compressor power with the mechanical losses

accounted for, while the power of the other turbine is equal to the effective power of GTE.

a)

b)   c)

Fig. 4 Aluminum model of turbine wheel for 60 KW tunnel turbine

a) General view; b) peripheral disc (stream inflow side); c) preaxial disc (stream outflow side).
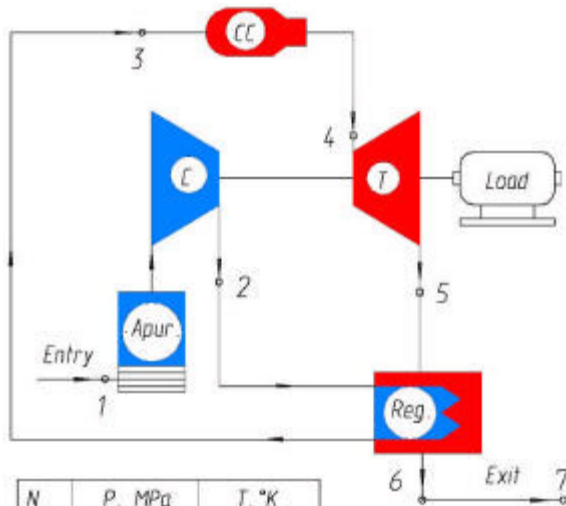

Fig. 5 Thermodynamic scheme with turbine stage of 60 KW power.

Table 1. Initial data and data of calculation of cycle of 6OKW GTE tunnel turbine stage.

N	NAME	Value
1.	**Initial data**	
1.1	Effective power, KW	60
1.2	Combustion products temperature at turbine inlet ^{o}C/^{o}K	1350/1623
1.3	Pressure ratio	4.0
1.4	Atmospheric pressure, MPa	0.1013
1.5	Atmospheric temperature, ^{o}C/^{o}K	15/288
1.6	Pressure conservation factor at inlet, %	98
1.7	Pressure conservation factor at outlet, %	98
1.8	Mechanical efficiency, %	99
1.9	Generator efficiency, %	97
1.10	Total relative leaks in cycle	0.005
1.11	Total relative air flow for cycle cooling	0.0150
1.12	Combustion completeness, %	99
1.13	Pressure conservation factor in combustor, %	96
1.14	Compressor efficiency, %	82
1.15	Turbine efficiency, %	81.2
1.16	Regeneration ratio	79.8
1.17	Pressure conservation factor for air, %	97.5
1.18	Pressure conservation factor for gas, %	95.5
2.	**Cycle calculation results**	
2.1	Air flow at combustor inlet,kg/s	0.249
2.2	Fuel flow, kg/s	0.034
2.3	Air excess coefficient	4.57
2.4	Compressor power, KW	44
2.5	Working media flow, kg/s	0.52
2.6	Pressure reduction ratio in compressor turbine	1.62
2.7	Compressor turbine power,KW	44
2.8	Working media flow at power turbine inlet, kg/s	0.256
2.9	Pressure reduction ratio in turbine	2.12
2.10.	Power turbine output,KW	61
2.11	Cycle efficiency, %	38.03

5. Geometry of the nozzle vanes and turbine wheel of the model tunnel turbine of GTE of 60KW

The geometry of the turbine wheel was calculated on the basis of the initial calculation parameters (see Table 1). As a result of multi-version approach with the simultaneous calculation of geometry and gas dynamics (see section 6) of the turbine wheel, the geometric sizes of the external contours, channel sizes and their position in the discs' body were identified. The turbine wheel consists of two discs, namely the main peripheral and near-axial ones, the latter twists the gas stream additionally at the wheel exit. The wheel is secured on the bearings in cantilever. The additionally twisting disc is joined with the main disc by 6 pins. At the wheel exit, a deflector is added to the additionally twisting disc. The channels are subdivided into three main groups of different geometry. The local system of coordinates for each channel begins in the point on the diameter $\varnothing$105, with equal spacing over the periphery. The determining angles and projection of the channel axes for each group of two coordinate systems (disc and channel) are shown in Fig.6 with their values shown in Table 2.

The calculation of the turbine wheel was performed in combination with guide vanes , i.e. a unique methodology was developed that allows, first, to optimize the guide vanes geometry in terms of obtaining the required gas-dynamic values and then carrying out an optimization calculation of the turbine wheel that would be best combined with the guide vanes.
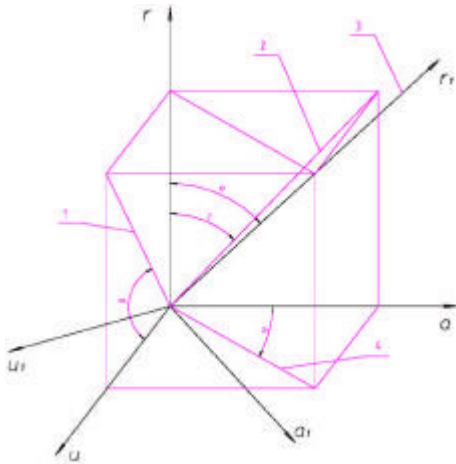
Fig.6 Determining angles and projections of axes of channels for each set of channels in the Cartesian system of coordinates for discs and channel.

a, r, u – system of disc coordinates;

a_1, r_1, u_1 – system of disc coordinates;

φ – angle of nutation;

ψ - angle of precession;

γ - angle between centerline (r) and projection of channel centerline on plane (ra);

β - - angle between centerline (u) and projection of channel centerline on plane (ru);

1 – projection of channel centerline on plane (ru);

2 - projection of channel on plane (ra);

3 - channel centerline;

4 - projection of channel centerline on plane (ua);

Table 2. Geometric parameters of nozzle vanes and turbine wheel of 60KW GTE tunnel turbine stage

N	Name	Value					
1.	**Nozzle vanes**						
1.1	NV inlet diameter,mm	130					
1.2	NVoutlet diameter, mm	105					
1.3	Angle of stream outflow from NV in pl (r u), degree.(fig.6)	17.50					
1.4	Angle of channel Inclination in NV in pl..(r a) at outlet, degree(fig.6)	30.0					
1.5	Number of channels., Pcs.	17					
2.	**Turbine wheel**	**Disc**					
		(1) peripheral			(2) nearaxial		
		Group of channels					
		1	2	3	1	2	3
2.1	Total number of Channels at inlet	33			33		
2.2	Number of channels Per group	11	11	11	11	11	11
2.3	Diameter of channels At inlet, mm	7.30	7.22	7.08	8.265	8.05	7.49
2.4	Channel length, mm	24.1	20.5	19.2	17.54	12.5	10.6
2.5	Radius for circle Of openings at Channel inlet , mm	52.50			32.50	37.3	42.3
2,6	Radius for circle of Centers of openings At channel outlet,mm	32.5	37.3	42.3	23.3	33.0	40.1
2.7	Angle of entry in pl.. (r u), ß$_1$, degree	70.5	7,05	70.5	59.0	41.0	21.3
2.8	Angle of exit in pl. (ru),ß$_2$, degree.	57.3	65.7	65.5	44.20	31.5	10.9
2.9	Angle γ, degree.	25.0	39.5	57.0	53.0	65.5	69.0
2.10	Taper	0.040			0.070		

It should be noted that the calculation was carried out with no limitations for those geometric parameters of the turbine wheel which changing would result in a considerable complication both of the software and, as the next step, the techniques to manufacture the turbine wheel. The like parameters, primarily, include: the inlet diameter of channel, spacing between the inlet openings of the channels, channel taper, shift along the longitudinal axis of inlet opening centers for the adjacent channels.

The multi-version calculations revealed that the limitations for variations of these parameters do not allow obtaining an optimum combination of the gas-dynamic and strength characteristics for the turbine wheel of the tunnel turbine.

6. Gas-dynamic calculation of the radial tunnel turbine
This new type of the radial turbines has no analogue in the history of the turbomachinery developments. Therefore, to calculate the like machines, a methodology of gas-dynamic calcPeriulations was developed with some basics as follows:

6.1 Bernoulli's and Euler's gas state equations are employed in the calculations to identify the specific turbine work, continuity, working media stream energy, isoentropic and polytropic processes.

6.2 At calculation, the 3-D kinetics of absolute and relative velocity vectors is admitted with use of both the natural (local) Cartesian system of coordinates and the general cylindrical system of coordinates.

6.3 Identification of the loss factor for the nozzle vanes channels path and turbine wheel is subdivided into the impact overflow losses, losses induced by the stream friction against the channel wall, stream turn in the turbine wheel at the discontinuity of the 1st and 2nd disc axes and the edge losses (exit).

6.4 Estimation of the impact overflow losses in the turbine wheel channels in the 1st approximation is performed similar to case with the axial turbine systems using the relative angle of incidence.

6.5 Identification of the friction loss factor is the same as that for the friction loss factor for tube referred to the exit velocity.

6.6 Stream turn losses in the nozzle vanes are not available since the channel is rectilinear while in the turbine wheel in the 1st approximation they could be estimated for tubes installed at an angle to one another.

6.7 Edge losses could be estimated also in a way similar to the case with the gas turbine systems by the effect of the relative thickness of the exit edge. It is necessary to find an equivalent relative thickness of the exit edge for the given turbine wheel. It could be expressed as

$$\underline{d}_{eq.}= 1 - \frac{F_{open}}{F_{comp}},$$

where

F_{open} is the open section of channel;

F_{comp} is the complete section normal to the channel axis, confined by the circumferential and radial boundaries of the adjacent channels.

6.8 Gas-dynamic calculation for each set of channels is performed separately with the final identification of work performed by each set of channels. Then these works are summarized.

As a result of the solution, the parameters for the stream along the tunnel turbine path, including the specific work of the nozzle vanes, absolute stream velocity at the nozzle vanes exit and its components, relative velocity at the turbine wheel inlet, pressure and temperature downstream of the nozzle vanes, stream parameters in the turbine wheel channels, turbine efficiency (Table 3) are identified.

Table 3. Gas dynamic calculation of 60 KW GTE tunnel turbine stage

N	NAME	Value		
1.	Extra initial data to Table1			
1.1	Total power, KW	108		
1.2	Power consumed on friction and Ventilation of turbine wheel, KW	3.1		
1.3	Rotor speed, rpm.	$110 \cdot 10^3$		
1.4	Pressure reduction ratio In turbine	3.43		
1.5	Reaction	0.100		
1.6	Roughness of channel surface, μm	1.6		
2.	Dynamic calculation results			
2.1	Nozzle vanes			
2.1.1	NV specific work.,kJ/kg	340.5		
2.1.2	Absolute velocity at NV outlet, m/s	794.3		
2.1.3	Corrected velocity at NV outlet.	1.09		
2.1.4	Static temperature at NV Outlet, ^{o}K	13.69		
2.1.5	Static pressure at NV outlet, MPa	0.168		
2.1.6	Density at NV outlet., kg/m^3	0.424		
2.1.7	NV channel length., mm	26.66		
2.1.8	Channel diameter at NV outlet.,m	7.62		
2.1.9	Pressure conservation factor in NV.	0.9383		
2.1.10	Loss factor in NV.	0.074		
2.1.11	Velocity factor in NV.	0.962		
2.1.12	Reynolds number at NV outlet.	50530		
2.2	Turbine wheel parameters			
2.2.1	Total rel. temperature at TW inlet., ^{o}K	1407		
2.2.2	Total rel. pressure at TW inlet., MPa	0.189		
2.2.3	Rel.angle of stream at TW inlet in pl.. (r u), degree.	58.9		
2.2.4	Rel.velocity at TW inlet., m/s	306.4		
2.2.5	Peripheral velocity at TW inlet, m	604.8		
2.3	Turbine wheel			
	Number of group of channels			
2.3.1	Specific work of group of channels, kJ/kg	425.2	392.5	428.7
2.3.2	Rel.velocity at inlet, m/s	425.9	428.2	446.2
2.3.3	Rel. velocity at inlet , m/s	413.9	463.4	500.9
2.3.4	Static temperature at outlet , ^{o}K	1220	1232	1245
2.3.5	Static pressure at outlet, MPa	0.092	0.092	0.093
2.3.6	Peripheral velocity at outlet, m/s	269	381	463
2.3.7	Absolute velocity at outlet, m/s	355.7	403.1	239.1
2.3.8	Corrected velocity at outlet	0.551	0.618	0.371
2.3.9	Channel diameter at outlet,mm	9.60	9.03	8.70
2.3.10	Angle of stream turn, degree.	70.136	94.538	104.908
2.3.11	Angle of incidence at inlet,degree	10.762	16.783	30.301
2.3.12	Stream friction loss factor *	0.000	0.000	0.000
2.3.13	Impact entry loss factor *	0.000	0.000	0.000
2.3.14	Edge loss factor *	0.000	0.000	0.000
2.3.15	Stream turn loss factor *	0.000	0.000	0.000
2.3.16	Loss factor in TW	0.31	0.328	0.344
2.3.17	Pressure conservation factor in T	0.895	0.861	0.830
2.3.18	Outlet density, kg/m^3	0.260	0.258	0.257
2.3.19	Flow in group of channels, kg/s	0.086	0.084	0.0084
2.3.20	Efficiency of group of channels	0.849	0.813	0.808
2.3.21	Reynolds number at TW outlet.	21571	22462	23201
2.4	Parameters at turbine outlet			
2.4.1	Adiabatic drop per turbin e, kJ/kg	504		
2.4.2	Total temperature at TW outlet, ^{o}	1279		
2.4.3	Total pressure at TW outlet, MPa	0.108		
2.4.4	Turbine efficiency by total Parameters	0.8240		
2.4.5	Polytropic turbine efficiency by total parameters.	0.8049		

- *In the 1st approximation to carry out the precalculations, the values presented here, are equal to zero, their actual values are to be identified by the experiments and accounted for at the final calculation of the turbine.

-

The results of the precalculations indicate that despite the complimentary values of losses were specified in the nozzle vanes and turbine wheel, the efficiency of the tunnel turbine is at the level typical for the current centripetal turbines. Thus, you can anticipate that the given type of turbines has the efficiency not inferior to that of the current structures.

7.Metal model of tunnel turbine stage. Model arrangement on the experimental rig

On the basis of the thermal-dynamical and gas-dynamical calculations accomplished, the metal model of the tunnel turbine stage was developed and manufactured, i.e. the nozzle vanes (Fig.2b) and turbine wheel (Fig4) that are the full-scale copies of these components of a real-scale tunnel stage.

The only difference is the material applied; thus, high-alloy heat resistant alloys and high-temperature materials on the basis of alumo-boron-nitride compositions will be used in the real-scale turbine (Soudarev,2002) while in the model there will be used the aluminum alloys of D16 type (tensile strength is σ_b=310 MPa,AK-4 (σ_b=416 MPa or AK-6 (σ_b=480 MPa). The density of these alloys is 2.8 g/cm^3, the Poisson factor is 0.31, elasticity modulus is $7.1 \cdot 10^{10}$ MPa.

The model stage is intended to estimate the effectiveness of the gas-dynamic characteristics of the tunnel turbine stage developed and it will be studied under "cold" conditions on the existing experimental rig where the radial ceramic turbines of a conventional design had been studied earlier. All the appropriate development and manufacture works to arrange the tunnel turbine stage and the existing test rig centrifugal compressor (Fig.7) within the casing and rotor elements of the experimental rig were performed (Fig.8).

The turbine arrangement is shown in (Fig.9). The turbine stage including the turbine wheel (1) and guide vanes (2) is within the double casing of the volute. The cover ring (9) that provides formation of the working media flow and decreasing of the air overflow from the gap between the turbine wheel and guide vanes by means of the labyrinth seals is mounted at the air outlet of the turbine wheel. The screen (6) is placed between the bearing housing and the turbine wheel to reduce the hydro-dynamical ventilation air losses in the annular space between the turbine wheel and the housing; in addition to its other functions, the diaphragm secures the guide vanes against a likely cranking using four studs (7).

To build up the maximum smooth flow of the working media into the guide vanes channels, the deflector in the form of tongue is placed inside the internal casing (3) of the volute. The flange (5) fixes all the parts by pressing them to the turbine casing.

Fig. 7 GTE rotor of 60 KW power (centrifugal compressor and tunnel turbine) after assembly and balancing.

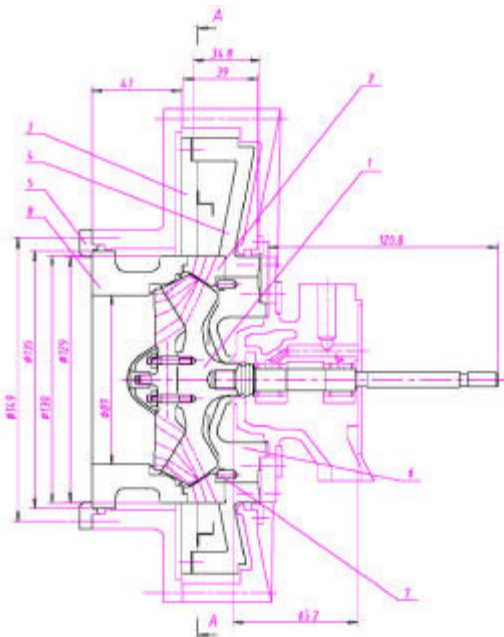Fig. 8 Rotor elements of the experimental rig

Fig. 9 Arrangement of model turbine stage on the experimental rig.

1 – turbine wheel; 2 – nozzle vanes; 3, 4 – volute walls; 5 – flange; 6 – screen; 7 – fixing pin; 8 – cover ring.

8. Identification of duties of gas-dynamic tests of the model turbine wheel of the tunnel turbine

The estimation of the effectiveness of the gas-dynamic characteristics of the model turbine wheel developed will be carried out at the "cold" tests, i.e. under inlet conditions different from the standard engine duties. Since in terms of geometry the model is fully similar to the real one, a prerequisite of the flows outlined above is equality of the corrected flows, referred rotor speed and corrected power. This is just under these conditions that the equal flow kinetics for both the real-scale and model turbine stages is maintained.

$$\overline{G} = \frac{G \cdot \sqrt{T_0^*}}{P_0^*} = const \tag{8.1}$$

$$\overline{n} = \frac{n}{\sqrt{T_0^*}} = const$$

$$\overline{N} = \frac{N_T}{P_0^* \cdot \sqrt{T_0^*}} = const$$

A difference between the working media characteristics (adiabat value K, universal gas constant R, etc) for the real scale and the model can be ignored.

In compliance with the conditions (8.1), the parameters $\overline{G}$ $\overline{n}$ and $\overline{N}$ at rating must have a corresponding pressure ratio in the turbine. Given the working media exhaust into atmosphere, the total pressure at the turbine inlet at rating will be

$$P_O^* = \pi_t^* \cdot P_{atm} = 3{,}435 \cdot 0{,}1013 = 0{,}348 \text{ MPa} \tag{8.2}$$

Then, the corrected parameters at rating will be

$$\overline{G} = 27{,}51 \; \frac{kg \cdot K^{0,5}}{C \cdot MPa} \quad , \tag{8.3}$$

$$\overline{n} = 2730 \; \frac{rpm}{min \cdot K^{0,5}} \quad , \tag{8.4}$$

$$\overline{N} = 0{,}00683 \; \frac{MW}{MPa \cdot K^{0,5}} \quad , \tag{8.5}$$

The flow across the turbine, rotor speed and power are determined on the basis of the selected initial temperature upstream of the turbine. The turbine inlet temperature must be chosen on the basis of the temperature level downstream of the turbine because of a likelihood of the stream's temperature getting colder at the outlet.

It should be noted that at the simulation in compliance with the conditions (8.1) of maintaining the gas-dynamic similarity, the Reynolds number varies. Typically, it increases proportionally to reducing $\sqrt{T_0^*}$ at the "cold" tests with the initial pressure at the turbine inlet maintained. If not to consider the value of the channel roughness, the friction loss factor in the real-scale and model turbines will keep decreasing by the Blazius law. Though these losses at the "cold" tests (model) will always be less those in the real-scale turbine with the relative roughness of the tunnel surface being not below 500. In this case, the friction loss factor is lower with the roughness effect being accounted for, i.e. it drops from 2.5 to 1.9 (24% decrease) while by the Blazius law it drops from 2.5 to 1.7

(32% decrease). Accordingly, the gas-dynamic efficiency of the turbine stage will change, too.

9. Strength calculation of the model turbine wheel as applied to the "cold" gas-dynamic rig tests

As follows from the above section, the rotor speed varies as a function of the air temperature at the turbine inlet at testing the real-scale turbine wheel on the "cold" gas-dynamic test rig. With the temperatures ranging 320 to $360^{0}C$ at the turbine wheel inlet, the rotor speed varies from 53500 to 57500 rpm (see Fig.10 and 11). The calculation of the stressed state for the peripheral and near-axial discs was performed for the speed of n=60000 rpm when they are made of the aluminum alloy.
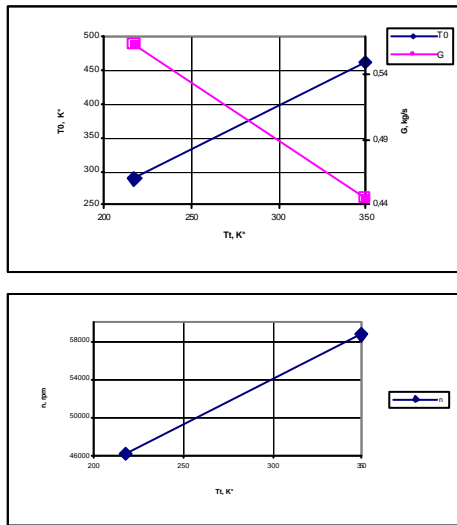

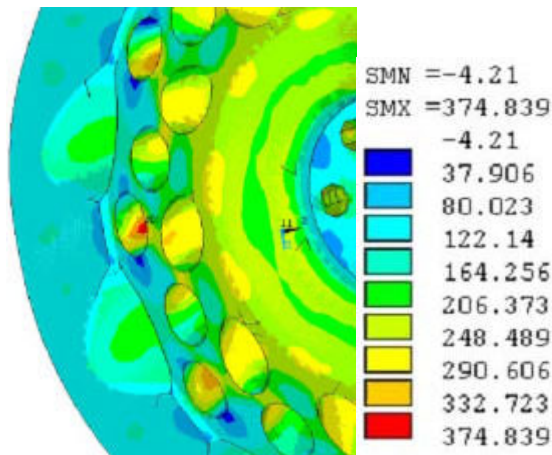Fig. 10 Temperature at turbine inlet and air flow in model turbine versus outlet temperature.

Fig. 11 Distribution of main stresses in the peripheral disc of the turbine wheel of the tunnel turbine stage.

The highest stresses were observed on the spots of the stress concentrators on the disc periphery in the holes and, also, an opening of the discs relative to each other took place due to a bending of the disc platforms under operation speed conditions.

Therefore, there was a need in carrying out a complex of calculations and design corrections to reduce the maximum stresses up to the level lower 400 MPa and to match the disc strains. The peripheral disc proved to be the most stressed one. To implement this target, a number of design changes was performed (milling-outs over the disc periphery, increase in the peripheral diameter, getting the disc neck thicker, alteration of the disc interface geometry, decrease in the boring depth, etc) which allowed more than twice reduction of the maximum stresses in the turbine wheel discs.

Distribution of the main stresses in the most stressed peripheral disc is shown in Fig.11. It is evident that the maximum level of stresses does not exceed 375 MPa. In the near-axial disc, it is even lower, namely 268 MPa. The disc opening at the same time is eliminated.

Thus, the design, engineering and material science activities accomplished along with the following update of the turbine wheel disc geometry ensure a robust structure which was verified by the "cold" tests.

10. Summary

10.1 **The concept** of a novel **turbomachinery type, named tunnel** where the functions of the annular gratings of the axial or radial nozzle vanes and turbine wheel are taken over by the annular **system of conic channels** –tunnels was proposed.

10.2 **A methodology of gas-dynamic and strength calculations** for the tunnel turbine stages was developed, it allowed to identify the design sizes and geometry of the nozzle vanes and the turbine wheel that ensure their efficient and reliable operation.

10.3 **A model of the tunnel turbine stage** was manufactured, it serves to identify the gas-dynamic characteristics of the stage under the "cold" tests conditions.

10.4 **An update of the experimental test rig** was carried out along with the adaptation of the manufactured turbine stage to the existing compressor, plausible operating conditions, etc.

REFERENCES

Dietz P., Scholz R., Gur M., and Morgenroth S, 1989, "Konstructive und betriebliche Probleme mit keramischen Werkstoffen beim Einsatz von Heissgasventlatoren", Kolloquim "Konstruktion verfahrens-technischer Maschinen", Clausthal-Zellerfeld, pp.183-219.

Elkins R.T.,1999, "Innovate design of ceramic utility gas turbines", "Trans. ASME J.Eng.Power", N 4, pp.556-562.

Gabrielsson R., Lundberg R., and Avran P., 1998, "Status of The European gas turbine program AGATA", 43rd ASME Gas Turbine and Aeroengine Congress, Stockholm.

Patent of France, 0210977 of 05.09.2002. 75, INPI Paris, Turbine a gas a roue de turbine de type radial.

Price J.R., Jimenez O., Parthasarathy V., Miriyala N., 1999, "Ceramic Stationary Gas Turbine Development Program - Sixth Annual Summary", ASME Paper 99-GT-351, International Gas Turbine and Aeroengine Congress and Exhibition, Indianapolis, Indiana.

Tatsumi T., Takehara J., Ichikawa J., 1999, "Development Summary of the 300 kW Ceramic Gas Turbine CGT302", ASME Paper 99-GT-105, International Gas Turbine and Aeroengine Congress and Exhibition, Indianapolis, Indiana.

Soudarev A.V.,Tikhoplav V.Yu,.2002, Ceramic Gas Turbine Design and Test Experience. Progress in ceramic Gas Turbine Development, ASME PRESS, edited by Mark van Roode, Mattison K., Ferber, David W.Richerson, Vol.1, chapter 32, pp.683-707.